Proceedings of the 2012 IFAC Workshop on Automatic Control in Offshore Oil and Gas Production, Norwegian University of Science and Technology, Trondheim, Norway, May 31 - June 1, 2012

A Hybrid Approach to Closed-loop Directional Drilling Control using Rotary Steerable Systems

J Matheus, M Ignova, P Hornblower

Schlumberger Technology Centre, Brunel Way, Stroud water Park, Stonehouse, Gloucestershire GL10 3SX, UK.

***Abstract*:** This paper proposes the use of a hybrid approach to perform the trajectory control in the oil drilling industry using Rotary Steerable Systems (RSS). Two levels of automation are proposed, the attitude control (Level 1) regulating inclination and azimuth downhole and the outer loop (Level 2), that monitors the performance of the inner loop and controls the directional drilling commands issued to the tool in order to follow a pre-defined plan. The attitude controller was developed using various simulation techniques including Hardware in the Loop, which implements the dynamical model of the regulated variables downhole. This approach guarantees the reliability of the embedded software implemented in the RSS tool.

Keywords: Trajectory Control, Hybrid Control, Drilling Automation, Rotary Steerable Systems

1. INTRODUCTION

The history of trajectory control can be traced back to the days of drilling with rotary assemblies, where experienced directional drillers who had specific knowledge about the response of bottom hole assemblies (BHA) in a particular area carefully picked bits and stabilizer placements in order to give the BHA the correct build and walk tendencies. This process required a lot of trial and error during the learning phase, resulting in many corrective runs and non-productive time. Moreover, the tendency of the BHA was not the same in all the wells drilled (Millheim et al., 1977, 1978).

Then came the age of drilling with motors and Measuring While Drilling (MWD) tools, with slide/rotate profiles often with a low rate of penetration (ROP) due to poor transfer of force to the bit during the slide sections (Baker, 2001). Due to the limitations in downhole and surface communications and the distance of the bit to the D&I package, the trajectory control actions performed by the Directional Drillers (DD's) resulted in tortuous well bore, see Fig.1.

With the advent of Rotary Steerable Systems (RSS), (see Downton et al., 2000), there was a natural increase in efficiency, mainly due to replacement of slide/rotate profiles with rotary drilling, with a more stable borehole and better hole cleaning. These advantages have pushed the envelope of drilling in the industry, and today, we have wells with step out of more than 40,000 ft from the drilling rig. As these tools are fully instrumented with sensors close to the bit, operators have been increasing their requirements in terms of precision trajectory control and trajectory placement at extended depths while geosteering. The ability to deliver these wells with precision has become mandatory in drilling practices today.

Many of the system trajectory models used for RSS have tended to be rather complex, and created with the aim of capturing the trajectory response of rotary steerable tools in high fidelity. To model the dynamics and kinematics of the system, several aspects have to be taken into account, for example, rock-bit interaction, steering mechanisms interactions with the formation, downhole vibrations. This has lead to the widespread use of the finite element methods to solve the drillstring bending and mechanism contact problems (see Pastsek et al., 2003, Fenoui, 1998 and Lesso and Chau, 1999).

Another example of modeling rotary steerable tools from a physical standpoint is presented in Downton and Ignova (2011), where starting from quasi-static force considerations, a delay differential equation and hence transfer function is derived describing the displacement, inclination and curvature response of a rotary steerable tool in terms of the position of the stabilizer contact points with respect to the formation, the flexibility of drill string members, bit machining model, self weight, axial load induced distortions, hole over gauge, actuator force and actuated lateral displacements to arrive at a closed algebraic expression for hole propagation – thus obviating the need to simulate drilling response in many cases and revealing the essential parameters governing system responses.

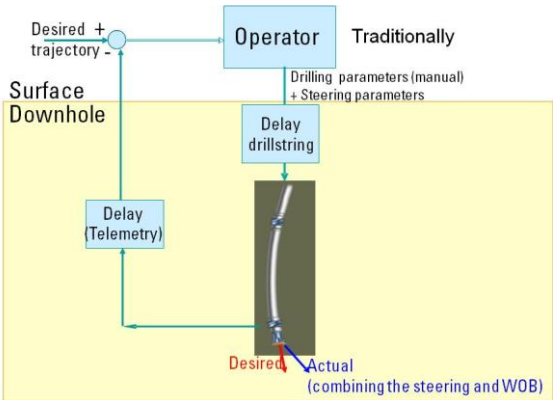

Fig. 1. Traditional drilling control.

Bayliss and Matheus (2008) derives a generic system model in 2D and 3D, which captures all the fundamental behavior of a drilling tool, where physics and formulation of the model is scalable in complexity so that the same principles can be used to implement large and complex drilling simulations. Then, linearization of the system model is performed and control algorithms are designed to regulate in a simulated environment the inclination of the drilling tool downhole.

This paper is organized as follows: The first part presents the process followed in the development of the RSS trajectory control algorithm, describing the structure of the mathematical models, the control strategy implemented, and the test methodology to evaluate the downhole firmware. The second part presents worldwide field tests results. The third part describes a generic approach to control the trajectory of a well specifying the different control layers that operate at different sampling times/measured depth intervals. Finally, the conclusion is including the lesson learned from the field trials.

2. DEVELOPMENT OF RSS ATTITUDE CONTROL ALGORITHM

2.1 Overview of the process flow

Fig. 2 shows the process followed in the development of the RSS attitude control algorithm.

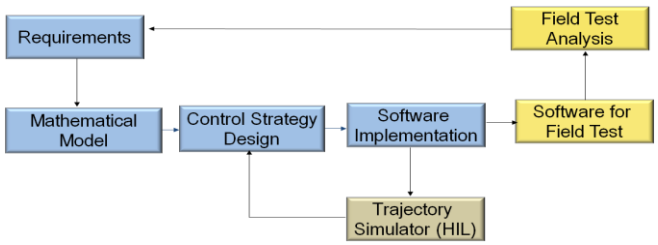

Fig. 2. Development phases of the RSS attitude control.

The process starts with the definition of the high-level requirements. Usually, the clients specify the TVD tolerance, length of the oscillations, inclination and azimuth tolerances. The second stage is the formulation of mathematical models that describe the dynamic evolution of the inclination and azimuth downhole, either using first principles or estimation theory models.

The third stage is to develop the control strategy to regulate the system's variables and states. In this stage, any of the following techniques can be used to design the control strategy, e.g. traditional control methods, modern control or heuristic control strategies.

The fourth stage is to develop or transform the control strategy to the embedded platform, usually coded in Assembler, C, or C++. Hardware in the Loop (HIL) techniques are often used to test the embedded implementation creating an attitude simulator to interact with the software and hardware, and to emulate the well propagation downhole.

Iteration of the control designs, software implementation and testing continues until the software implementation is demonstrated to have fulfilled the high level requirements.

The last stage is the analysis of the field test results, comparing the simulation results with the real data obtained in the field tests. If needed, new requirements are formulated, and the process starts again.

2.2 Modeling for trajectory control design

A typical trajectory profile (plan) that the RSS tools are engaged to drill is graphically presented by Fig. 3. The actual drilled trajectory profiles are measured in real time using the accelerometer and magnetometers from which the inclination and azimuth are obtained. The mathematical equations for the inclination and azimuth including the uncertainties as well as the spatial delays due to the position where these measurements take place are included in the subsection below.

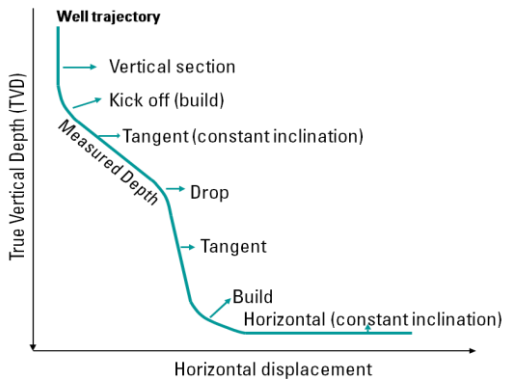

Fig. 3. Representation of the trajectory profile (2-D example).

The continuous inclination (C_Inc) and azimuth (C_Az) used in the closed-loop control algorithms are calculated using (1) and (2):

$$C\_Inc = \text{acos}\left(\frac{G_z}{G_{tot}}\right) \tag{1}$$

Where: $G_{tot} = \sqrt{G_x^2 + G_y^2 + G_z^2}$, is the earth gravity close to 1 g.

$$Num = \sqrt{\left(1 - \frac{G_z^2}{G_{tot}^2}\right) \cdot \left(1 - \frac{B_z^2}{B_{tot}^2}\right) - \left(sinDip - \frac{G_z \cdot B_z}{G_{tot} \cdot B_{tot}}\right)^2}$$

$$Den = \frac{B_z}{B_{tot}} - \frac{G_z \cdot SinDip}{G_{tot}}$$

$$C\_Az_{(Bz,Gz)} = \frac{180}{pi} atan\left(\frac{Num}{Den}\right) \tag{2}$$

Where: *SinDip* is the *sin* of the dip angle, G_z is the normalized accelerometer value and B_z is the normalized magnetometer value in the axial direction.

The uncertainty in the calculations of the azimuth and inclination are presented in equations (3) and (4):

$$\sigma_{C\_Az}^2 = \left(\frac{\partial C\_Az}{\partial B_z}\delta_{Bz}\right)^2 + \left(\frac{\partial C\_Az}{\partial G_z}\delta_{Gz}\right)^2 \tag{3}$$

$$\sigma_{C\_Inc}^2 = \left(\frac{\partial C\_Inc}{\partial G_z}\delta_{Gz}\right)^2 \quad (4)$$

Assuming that the magnetometers have an accuracy of 1000 nT and the accelerometers have 2mG, and evaluating the partial derivatives at different inclination the accuracy for the continuous azimuth is given by Table 1.

Equations (3) and (4) are for deriving the inclination and azimuth at the drill bit, however the measured inclination and azimuth are performed some distance behind the drill bit, therefore a spatial transport delayed is also added to the model as given by (5):

Table 1. Continuous azimuth accuracy (σ LEVEL) at different inclinations

Inclination (deg)	Azimuth (deg)
20	5.2
50	2.36
90	2

$$Inc^* = C\_Inc \cdot e^{-s \cdot T_d}$$

$$Az^* = C\_Az \cdot e^{-s \cdot T_d} \quad (5)$$

Where: Inc^* is the measured inclination; Az^* is the measured Azimuth; T_d is the transport delay defined as a distance between the bit and the inclination and azimuth measurements/ROP. Equation (5) represents the variable transport delay between the bit and the sensor due to the variations in the ROP. This type of dynamic is very complex to regulate and requires special considerations when designing control strategies.

2.3 Modeling for trajectory control design

The models to describe the behavior of the drillstring downhole and the rock-bit interaction have tended to be highly complex. A finite element analysis (FEA) model called "ST2" developed by Schlumberger calculates the trajectory of a well formed using a defined BHA, bit, and steering unit forces. For the control purposes, it is more convenient to approximate this with a transfer function that captures the main dynamics of the system under investigation. Advances have been made with respect of developing such a transfer function based on the delay differential equations (DDE) (see Downton, 2007), where a good agreement with the ST2 model has also been demonstrated.

An open approach has been followed to model the dynamics of the inclination and azimuth downhole. Instead of trying to describe the exact dynamics of the process, a set of equations are proposed where phenomenological models mimic the dynamics of the system. The equations used to describe the evolution of the inclination and azimuth downhole can be represented by ordinary differential equations, or by mathematical models obtained by the use of input-output correlations, such as neural networks or polynomials correlations.

Equations (6) and (7) describe the continuous evolution of inclination and azimuth downhole, these depends of the rate of penetration (ROP), tool dogleg severity (DLS), Toolface (TF), Steering Ratio (SR), DR (Drop Rate), and Walking Rate (WR), and parameters α, β, determined using historical data.

Equation (8) describes a mathematical relationship between the Toolface (TF) as function of the Toolface desired (TFD) (8).

$$\frac{dInc}{dt} = ROP \cdot \left(SR \cdot DLS_{\max} \cdot \cos(TF)\right) + DR \quad (6)$$

$$\frac{dAz}{dt} = \frac{ROP \cdot \left(SR \cdot DLS_{\max} \cdot \sin(TF)\right)}{\sin(Inc)} + WR \quad (7)$$

$$\frac{dTF}{dt} = \frac{1}{\lambda}\left(TFD - TF\right) \quad (8)$$

Where: λ – tool face response time; SR – steering ratio; DLSmax – Maximum DLS for tool; TF - toolface command; DR – drop rate; WR – walk rate; Inc – Inclination; Az – Azimuth; TFD– Tool face desired; ROP –rate of penetration.

For the purpose of this work all of the tool response and hole propagation effects are lumped into the toolface response time. Future work will involve the incorporation of more advanced representations, for example use of the delay differential equation approach (see Downton, 2007).

2.3 Attitude Control Design

Fig. 4 shows the block diagram for the RSS tool attitude control. It can be seen as two separate control loops run in parallel, one that controls the inclination (hold-the-inclination), and a second that controls the azimuth (hold-the-azimuth). The target inclination and azimuth are set by a downlink command and then the control strategy will continuously sample the inclination (*C_Inc*) and azimuth (*C_Az*). These two variables will be compared with the target inclination and target azimuth. A nonlinear control strategy, defined by the function "*f* " is implemented in the RSS Control Unit and produces the desired toolface and steering ratio which act as the commands to the RSS steering mechanism. The toolface is the direction to drill and the steering ratio is the percentage of time time that the RSS will spend in holding the desired toolface.

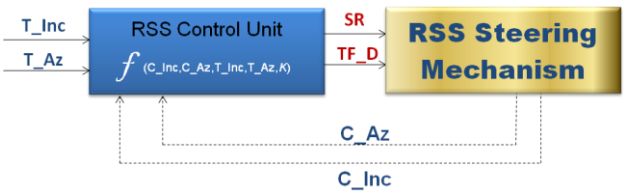

Fig. 4. Block diagram for RSS attitude control.

We can define a 2-D space with the co-ordinate system defined as the Azimuth on the X axis and the inclination on the Y axis. The target operational point can be represented as the point (Az_Des, Inc_Des) in this 2-D space. The current operational point at the Kth instant can be represented as another point (Az(k), Inc(k)) in this 2-D space. See Fig.5 for a picture representation. Let D_inc be the difference between

the desired inclination (*Inc_Des*) and the current Inclination (*Inc(k)*). See equations (9) and (10). Let *D_Azi* be the difference between the desired azimuth (*Az_Des*) and the current azimuth (Az(k)). Let Magnitude be the magnitude of the 2-D vector composed by (*D_inc*, *D_Az*), as represented by (9) and (10):

$$D\_Inc = Inc\_Des - Inc(K) \tag{9}$$

$$D\_Az = Az\_Des - Az(K) \tag{10}$$

Defining the Toolface as the direction to steer from the current operational point (*Az(k),Inc(k)*) to the target operational point (*Inc_Des*, *Az_Des*),), this is equivalent to the angle between the steering vector and the Y axis, see fig. 5. Fig. 5 shows the concept of the Steering Areas imposing ellipses as the shape of each area. This particular shape is very useful because for operational reasons it is often more important to control inclination than azimuth.

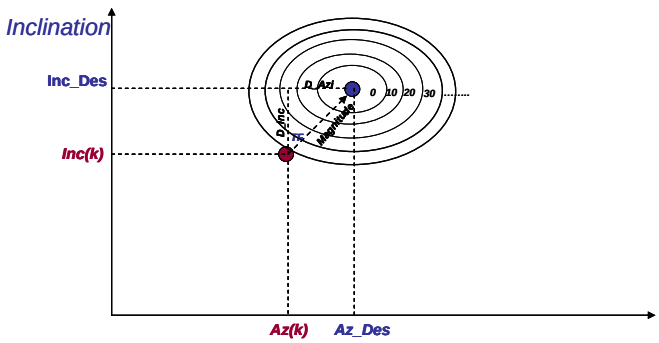

Fig. 5. Concept of the steering control.

2.4 Application of HIL for testing the RSS trajectory control algorithm

Fig. 6 shows the architecture of the hardware in the loop system used to test the RSS trajectory control algorithm. Its main parts are described as follows:

GUI: The user sets the target inclination; azimuth, and collar rotation in the simulator. Using this application the users can also inject perturbations to the system to evaluate the response of the trajectory control algorithm.

Trajectory Simulator: This contains the simulation of the hole propagation process and includes the evolution of inclination and azimuth as obtained from the differential equations defined in equations 6 - 8. This also includes emulation of the inclination and azimuth measurement process by defining the magnetic and gravitation field vectors as a function of simulated inclination, azimuth and collar rotation (equations 1 and 2). The control actions issued by the embedded controller are obtained using a proprietary low power tool bus (LTB) protocol.

RSS Low Voltage Electronics: This is the embedded platform composed of a sensor interface board, one DSP to perform the acquisition of the sensor raw data signals, one motor control DSP, and a CPU. The trajectory control firmware is implemented in the CPU, the control algorithm computes, the required toolface and steering ratio, depending of the actual inclination and azimuth.

Fig. 7 shows the output of the trajectory simulator controlled in closed loop with the RSS control algorithm. The simulation was performed assuming that the ROP is a normal distribution with mean 200 m/hr (650 ft/hr), and variance of 50 m/hr (160 ft/hr). The Dropping Rate (DR) was modeled as normal distribution with mean 1°/30m (1°/100ft) and variance 0.5°/30m (0.5°/100ft). Under these conditions the algorithm can control the inclination in ±0.2°, with very small oscillations.

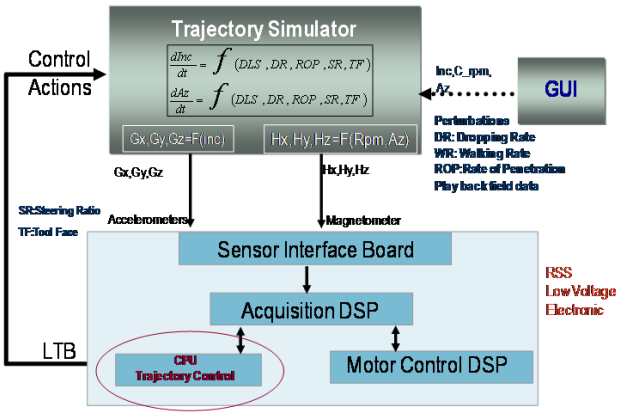

Fig. 6. Architecture of the RSS trajectory simulator (H need changing to B).

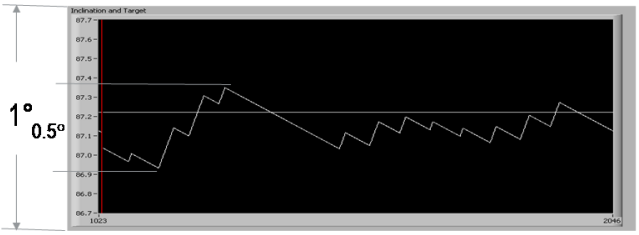

Fig. 7. Close loop response of the simulator.

Fig. 7 shows the output of the trajectory simulator when a large disturbance is injected in the control of the inclination. The first ellipse reflects the introduction of a large perturbation in the inclination, the variable changes from 87.2 to 86.0. The second ellipse shows the reaction of the RSS control to reject the perturbation.

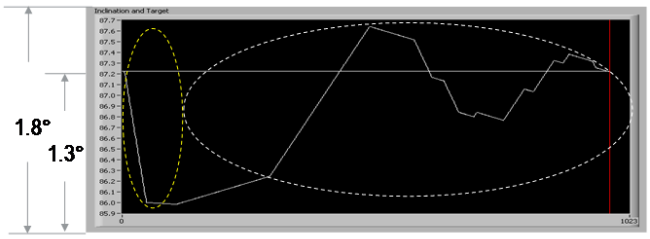

Fig. 8. Simulating an inclination disturbance in the RSS trajectory control simulator.

Fig. 8 shows the output of the trajectory simulator when two disturbances are introduced in the inclination and azimuth during the first 200 seconds of simulation. In this figure, it

can be seen how the RSS trajectory algorithm simultaneously regulates both inclination and azimuth.

3. FIELD TEST RESULTS FOR ATTITUDE CONTROL

3.1 Delivering Tight TVD Tolerance Wells with Powered RSS

The challenge of this drilling job was to deliver the well trajectory within the pay zone in a very tight TVD window of 0.5 m (1.6 ft). Additionally, the operator wanted to use a BHA with a positive displacement motor above the RSS, which increases RPM and so improves the RoP. In order to bring the RSS tool parameters to the surface in real time, a wireless communication device was also used that delivered all the inclination and azimuth related data to the surface as well as the tool status information while drilling ahead.

Fig. 9 shows the result of the RSS trajectory control algorithm, whereby the target TVD was maintained with a window of ±0.2 m (0.65ft). Three events are highlighted in this figure; the first is the activation of the RSS trajectory control at depth x400 m, between this depth and x620 m the inclination was changed from the surface to reach the desired TVD. The second event occurred at depth x620 m, at this point the well profile was matching the pre-defined well plan; however the geologist requested that the target TVD be lowered by in 0.2 m (0.64 ft). This is a common occurrence when drilling in the pay-zone and hence the target inclination again had to be adjusted in order to bring the TVD to the new target.

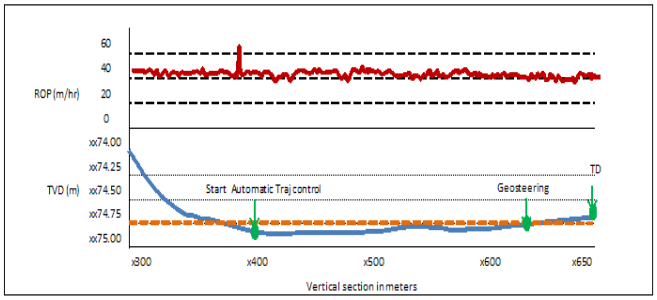

Fig. 9. TVD held in ±0.2 m (0.65 ft) using RSS Trajectory Control algorithm.

The final event occurred at depth x650 m, when the well placement engineers decided to declared target depth (TD), in other words stop drilling. The ability to control the TVD within these tight tolerances and also correct the trajectory to within ±0.1° has proven the accuracy and precision of the trajectory control algorithm.

Controlling Inclination at high ROP.

One particularly challenging aspects for any control strategy is its response under high speed conditions, as this generally implies higher frequency disturbances that exercise the system close to and sometimes above its bandwidth. Fig. 10 shows the performance of the RSS trajectory control algorithm in a very challenging field test, drilling at very high rate of penetration at 100 – 200 m/hr (320 – 650 ft /hr). The trajectory control was configured with the appropriate control gains to drill in high ROP. The client required control of the continuous inclination to within ±0.5° of the target inclination. Fig. 10 shows the 620 m section of the run where the target inclination was changed 3 times from the surface.

During the entire interval, the continuous inclination was always within the ±0.2° of the target. It is important to highlight that during the change of the target inclination in 1° at depth x870 m the close loop reaction of the tool reached the steady state value in 30 m (100 ft) with an overshoot of just 0.1°.

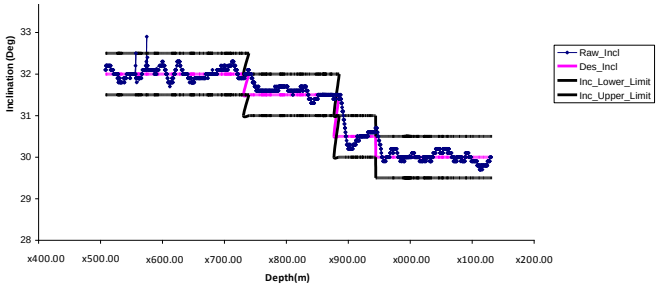

Fig. 10. Inclination control at high ROP.

4. THE HYBRID APPROACH TO CLOSE-LOOP TRAJECTORY CONTROL

As discussed in section II, the inclination and azimuth control automatically adjusts the steering commands and toolface by comparing the measured and the target inclination and azimuth. This forms the inner loop of a cascaded control system and runs at relatively high sample rate compared to the outer loop controller. The outer loop provides the set points, target inclination and target azimuth, for the inner loop in order to maintain the required trajectory. The trajectory loop can operate in two modes: Geometrical, correcting for TVD loss during transients as the inner loop attempts to reject disturbances and geological: changing the target TVD due to the uncertainty of the geological model and typically requested by the geologist or well placement engineers.

Fig. 11 shows the outer loop running every 90 feet and performing geological corrections by changing the target TVD according with a predefined well profile. Fig.12 shows a generic approach for the automation of the well placement based in Ignova et al (2010), several layer of control are proposed: (1) Formation that represents the hole propagation measured using accelerometers (Acc's) and magnetometer (Mag's) and it is affected by the steering force and desired toolface; (2) Control Unit/Steer Unit that represents the first level of control, computes the toolface based on sensors (Acc's) and (Mag's) compare them with Target TF and SR and execute the steering force to modify the formation level; (3) Attitude Control that represents the second level of control, it sense the continuous inclination and azimuth and computes the target TF and SR to be executed by the first level of control (4) Trajectory Control, which represents the third level of control, it sense the continuous vertical displacement (C_VD) and continuous horizontal displacement (C_HD) and computes the target Inclination and Azimuth to be executed by the second level of control.

GeoSteer/Well Placement: Represents the fourth level of control, it could execute complex reservoir models to maximize the well placement, and specifies the target vertical displacement (T_VD) and target horizontal displacement (T_HD) to be executed by third level of control.

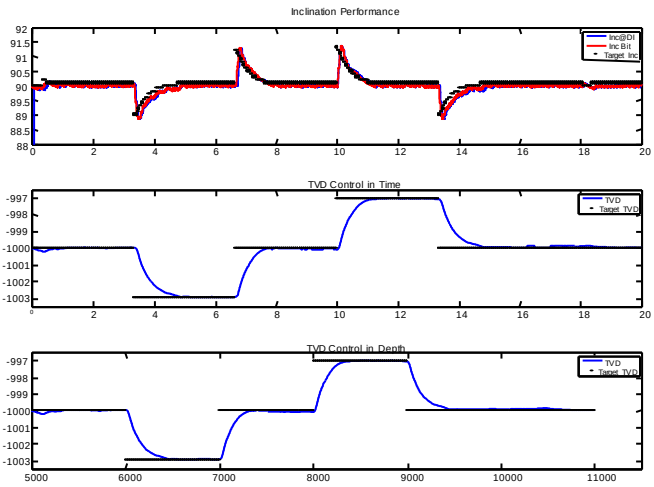

Fig. 11. TVD control operating in Geological Mode.

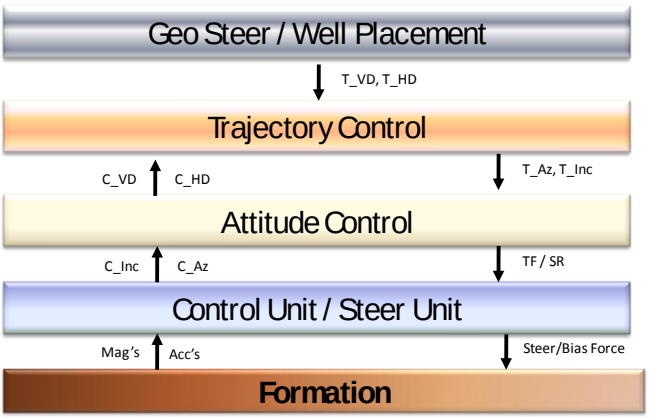

Fig. 12. Generic Automation for Well Placement.

5. CONCLUSIONS

Productive drilling is essential in today's Oil and Gas industry. There are many initiatives to increase the footage drilled per day but of equal importance is ensuring the optimal well placement. This is especially true in the pay-zone where deviations and errors in well bore trajectory can result in less than optimal flow rates in the producing well, reduced reservoir exposure if the well exits the reservoir or poor response to geo-steering commands, or even loss of the well if the trajectory enters the water table.

The results from the field trial of the Level 1 closed loop Inclination Hold (IH), Hold Inclination and Azimuth (HIA), Hold Inclination while Turning (HIT) in all types of well profiles, BHA configurations and ROPs show that the control strategy shows high levels of precision and robustness, as well as reducing well tortuosity and therefore torque and drag (an important part of extended reach drilling). Its contribution to the overall end game objective of increased productivity has been proven. As shown by simulations the addition of an outer loop to control TVD and reject errors, uncertainties and disturbances that cannot be detected and corrected by the Level 1 controller only operating in isolation has been demonstrated.

ACKNOWLEDGMENT

The authors would like to express our appreciation and are grateful to Schlumberger Oilfield Services for their continuous support and permission to publish this paper. We would also like acknowledge the contributions of our field personnel for providing valuable field test feedback and case studies during the execution of the project.

REFERENCES

Baker, R. (2001). A *primer of oilwell drilling*. 6th Ed., Publ. Petroleum Extension Service, Austin Texas.

Bayliss, M. and Matheus, J. (2008). Directional drilling tool simulation and system design. *SAE Int J. Mater. Manuf.*

Downton, G., Hendricks, A., Klausen, T. S. and Pafitis, D. (2000). New directions in rotary steerable systems. *Oilfield Review*, vol. 12, issue 1, 18-29.

Downton, G. (2007). Directional drilling system response and stability. *IEEE Multi-conference on Systems and Control*, Paper WeC06.3.

Downton, G, Ignova, M (2011). Stability and Response of Closed Loop Directional System using Linear Delay Differential Equation. *IEEE International Conference on Control Applications, Denver, 28-30 September.*

Fenoui, R. (1988). A microcomputer program for prediction of bottomhole assembly trajectory. *SPE Drill. Eng.*; Vol/Issue: 3:2.

Ignova, M., Downton, G. and Pirovolou, D. (2010). Directional drilling control devices and methods. Pub. No. US 2010/0175922 A1.

Lesso W. G. and Chau, M. T. (1999). Quantifying bottomhole assembly tendency using field directional drilling data and a finite element model, *SPE 52835, SPE/IADC Drill. Conf.*, Amsterdam, 9-11 March.

Millheim, K., S. Jordan, S. and Itter, C. J. (1978). Bottomhole assembly analysis using the finite element method. *Jr. Petro. Tech.*, pp 265 – 274.

Pastsek, P., and Brackin, V. (2003). A model for borehole oscillations. *SPE 84448*, Oct 5-8.